SOLUTION FREQUENCY-BASED PROCEDURE FOR AUTOMATED REGISTRATION OF TERRESTRIAL LASER SCANS USING LINEAR FEATURES

Kaleel Al-Durgham, Ayman Habib, Mehdi Mazaheri
Department of Geomatics Engineering, University of Calgary,
2500 University Drive NW, Calgary, Alberta, T2N 1N4, CANADA
kmaldurg@ucalgary.ca, ahabib@ucalgary.ca, m.mazaheri@ucalgary.ca

ABSTRACT

Over the last decade, terrestrial laser scanner systems have been proven to be an effective tool for the acquisition of 3D spatial information over physical surfaces. Many factors such as the low cost and the ability of rapidly collecting dense and accurate spatial data led to the utilization of laser scanners in different applications such as industrial sites modeling, 3D documentation of buildings, and many civilian and military needs. Usually, a complete 3D model for a given site cannot be derived from a single scan. Therefore, several scans with significant overlap are needed to cover the entire site and also to attain better information about the site than what could be obtained from a single scan. However, the collected scans will be referenced to different local frames that are associated with the individual scanner locations. Hence, a registration process, which aims at estimating the 3D-Helmert transformation parameters, should be established to realign the different scans to a common reference frame.
This paper introduces a new methodology for the automatic registration of terrestrial laser scans using linear features. Linear, cylindrical, and pole-like features are directly extracted from the scans through a region-growing procedure. Hypothesized conjugates of linear features are identified using invariant separation characteristics such as spatial separation and angular deviation between two linear features. All the hypothesized conjugate pairs – taken one at a time – are used to estimate the 3D-Helmert transformation parameters that are required to realign one scan to the reference coordinate system of another scan. Logically, only the right conjugate pairs among the hypothesized matches will lead to similar solutions of the transformation parameters. Therefore, we developed a strategy to detect the most frequent set of estimated parameters. A linear mathematical model that utilizes quaternions to represent rotation angles is used to simplify the estimation of the transformation parameters. Experiments will assess the performance of the proposed methodology over multiple scans of a power plant.

KEYWORDS: LiDAR Registration, Linear Features, Automatic Registration

INTRODUCTION

A registration process aims at estimating the 3D-Helmeret transformation parameters that describe the absolute orientation parameters between the involved scans. The 3D-Helmert transformation parameters include three rotation angles, three translations, and a scale factor. For a well-calibrated laser scanner, the scale factor is considered unity since the laser ranges provide the true scale. According to Habib and Al-Ruzouq (2004), a registration process should address four issues: (1) The registration primitives are the conjugate features within the scans that can be used to solve for the transformation parameters. These features could be points, 3D lines, and/or planes; (2) The transformation parameters relating the reference frames of the involved datasets; (3) The similarity measure, which is the mathematical constraint that describes the coincidence of conjugate features after the registration process; and (4) The matching strategy, which represents the guiding framework for the automatic registration process. Based on the final accuracy, the registration methods can be divided into either coarse registration techniques or fine registration techniques (Matabosch et al., 2005). The coarse registration techniques are used to establish the rough alignment between the involved scans. While the fine registration techniques are usually employed to achieve the precise alignment between the involved scans.

Direct georeferencing, target-based, point-based, or feature-based methods represents the different possible alternatives to achieve the registration of overlapping terrestrial laser scans. Each of these various alternatives has its own target function, advantages, and disadvantages. In the direct georeferencing methods, additional sensors such as GNSS and INS are combined with the laser scanner. Integrated GNSS/INS units are used to derive the absolute position and orientation of the laser scanner relative to the mapping frame and thus establish the coarse alignment between multiple laser scans. The direct georeferencing methods are applicable for mobile laser scanners (Asai et

al., 2005) and static terrestrial laser scanners (Scaioni, 2005). Due to the fact that the incorporation of direct georeferencing sensors impose additional expenses to the scanning system, the direct georeferencing methods are not preferable for most of the static terrestrial laser scanning applications.

Target-based methods utilize artificial targets for the registration of terrestrial laser scans (Liang et al., 2014). Typically, specially designed targets are involved to allow for their automatic recognition from the laser scans. A human effort is required to localize the targets within the scanner field of view, which can be restricted by the field access limitations. In addition, the initial alignment between the involved scans is manually achieved by visualizing the scans using a commercial software.

Point-based methods use the raw laser points to achieve the fine alignment between the overlapping laser scans. For instance, the well-known Iterative Closest Point (ICP) (Besl and McKay, 1992) is the most leading point-based registration algorithm. The ICP minimizes the point-to-point distance in the overlapping area between the different scans and iteratively estimates the transformation parameters. Variant derivatives of the ICP were introduced in the literature to increase its applicability to situations where there is no point-to-point correspondence. For instance, the Iterative Closest Patch (ICPatch) (Habib et al., 2010), and the Iterative Closest Projected Point (ICPP) (Al-Durgham et al., 2011) are examples of the ICP alternatives. All of the aforementioned point-based approaches have been proven to be effective in terms of accuracy. However, point-based registration methodologies require accurate initial approximations of the transformation parameters to establish the correspondence among conjugate primitives. In other words, point-based registration approaches should start from very good approximations of the transformation parameters (Chen and Medioni, 1992). Therefore, a wide variety of research efforts have been focusing on automating the initial alignment (i.e., coarse alignment) between the laser scans as a preparatory step to perform the point-based registration algorithms. Matabosch et al. (2005) surveyed several techniques such as Spin Images, Point Signature, and the RANdom SAmple Consensus approach (RANSAC) for identifying possible congruent points, curves, or surfaces. These techniques are computationally expensive since the feature extraction process requires transforming the raw point cloud into another domain (i.e., images, or meshes) and then further steps are required to find matching features.

The feature-based registration algorithms utilize geometric features such as lines, planes, spheres, and other higher order features to establish the coarse alignment between the laser scans. These features can be directly recognized and they provide a strong link between the laser scans. In this regard, one has to mention that the selection of the suitable registration feature is dependent on its existence within the scene. Rabbani and vanden Heuvel (2005) used planes, cylinders, and spheres as registration features. Their methodology of finding possible conjugate features was complemented by geometrical constraints. Jaw and Chuang (2008) have shown that linear and planar features offer reliable accuracy for the registration of neighboring laser scans. The most comprehensive work for automating the laser data registration using linear and planar features was proposed by (Yao et al., 2010), they developed a RANSAC algorithm to register laser scans in a pairwise fashion (i.e., two scans at a time). Their algorithm is based on measures that describe the shape and distribution of groups of linear and planar features in 3D space. It is reported that this method is sensitive to the presence of repetitive patterns, and the results of outdoor scene registration usually failed.

This research is dealing with the automatic registration of terrestrial laser scans using linear features. To address this topic, we stared with a brief review of relevant literature. Afterwards, the proposed methodology for using linear features to establish the automatic registration framework is outlined. The proposed methodology is then evaluated in the experimental results section. Finally, the paper presents some conclusions and recommendations for future work.

PROPOSED METHODOLOGY

This section explains our proposed methodology for the automatic registration of overlapping scans that contain several of linear features. We are using linear features to establish the coarse alignment between the overlapping laser scans. The linear features are directly extracted through a region-growing segmentation approach. Hypothesized conjugate pairs of linear features in two overlapping laser scans are identified by calculating the spatial separation and angular deviation between all the existing line pairs in each scan. Each hypothesized conjugate pairs are used to solve for the transformation parameters through a linear mathematical model. We proposed a process to determine the most frequent set of transformation parameters. Thereafter, the most frequent set of transformation parameteres is refined through an ICPP registration procedure.

Linear Features Extraction

A region-growing approach is developed for the direct extraction of pole-like features from terrestrial laser scans, where these features appear as cylindrical/ linear objects in the laser scanning data. First, in order to determine seed points that are used to start the region-growing approach, Principal Component Analysis (PCA) is performed over the local 3D neighborhood of each individual laser point. We define a local neighborhood to enclose the required number of points for reliable cylinder/3D line definition (e.g., nearest 50 laser points). The geometric nature of the point cloud within the established neighborhood is then investigated through eigenvalue analysis of the dispersion matrix of the neighboring points relative to their centroid. For the local neighborhoods enclosing a cylindrical/linear feature, one of the eigenvalues will be quite larger compared to the other two. The eigen vector corresponding to the largest eigen value provides the approximate direction of the pole-like feature. The other initial characteristic attributes describing the feature (e.g., location of a point along the feature and the radius of the cylinder) are then estimated while considering the local point density variation. Second, the points that are identified as belonging to a pole-like neighborhood are used as seed points to start the region-growing process. Starting from a single seed point, the neighboring points which belong to the same feature will be sequentially identified by checking point-to-line/cylinder axis normal distance. The 3D line/cylinder parameters that are associated with the seed point are refined iteratively using a least squares fitting procedure. We utilize the minimum parameterization of linear/cylindrical features that was introduced by Lari and Habib (2013) to avoid singularities during the fitting process. Finally, the points in a single feature are projected onto the line/cylinder axis to determine the extreme points. Afterwards, the ending points are used as descriptors of the linear features within the scan.

Identifying Hypothesized Conjugates of Line Pairs

The conceptual basis for the identification of conjugate linear features in two neighboring scans is figuring out invariant characteristics among conjugate linear features. First, the angular deviation between two lines is invariant to shift, rotation, and scale differences between two neighboring scans. Figure 1.a, shows the angular deviation (θ) between two 3D lines (e.g., $\vec{\imath}$ and $\vec{\jmath}$). Secondly, in the absence of scale differences between two neighboring scans, the spatial separation between lines $\vec{k}$ and $\vec{l}$ in Figure 1.b is invariant to shift and rotation differences. The spatial separation (S) represents the length of the common perpendicular line between two lines in 3D.

(a) (b)

Figure 1. Angular deviation (a) and spatial separation (b) between two lines in 3D

The angular deviation and spatial separation values between all pairs of lines in a given scan are used to identify potential conjugate linear features in overlapping scans. Therefore, if we have n linear features in the first scan and m linear features in the second scan, we will have $n \times (n-1)/2$ and $m \times (m-1)/2$ angular deviations and spatial separations that we need to estimate in these scans, respectively. Then, we need to identify the line pairs in both scans that have the same angular deviation and spatial separation. In this case, "same" means that they have similar values within a predefined threshold. This threshold depends on the noise level in the data as well as the accuracy of the feature extraction procedure. If the angular deviation and spatial separation between lines $\vec{\imath}$ and $\vec{\jmath}$ in the first scan are similar to those between lines $\vec{k}$ and $\vec{l}$ in the second scan, one can make a hypothesis that these line pairs are conjugate to each other. However, there will be two ambiguous matches for this case (i.e., line $\vec{\imath}$ in the first scan could be conjugate to either line $\vec{k}$ or line $\vec{l}$ in the second scan while line $\vec{\jmath}$ in the first scan would correspond to either line $\vec{l}$ or line $\vec{k}$ in the second scan). Due to the fact that a hypothesized match between two pairs in the two scans is equivalent to two possible matches between the individual linear features, the total number of possible matching line pairs from different scans will equal the number of lines combinations in the first scan multiplied by twice the number of combinations in the second scan according to Equation 1.

$$\text{Np} = n(n-1) \div 2 \times m(m-1) \quad (1)$$

Where, Np is the number of possible matching pairs.

Solving for the Transformation Parameters

A 3D linear feature has four degrees of freedom (Roberts, 1988). Therefore, a single straight line that could be identified in two terrestrial laser scans allows for the estimation of four transformation parameters relating these scans (i.e., the two shifts across the line direction and two rotation angles defined by the line direction). Another parallel line would allow for the estimation of the relative scale between the two scans as well as the rotation across the lines (i.e., the seven transformation parameters with the exception of the shift along the lines' direction can be estimated using two parallel lines). Two coplanar and non-parallel lines would allow for the estimation of the three shifts and three rotation angles among the two scans (i.e., only the scale parameter cannot be estimated using such lines). Therefore, two non-coplanar lines which can be identified in both scans will allow for the estimation of the relative scale, three shifts, and three rotation angles between the two scans. Thus, considering that there is no relative scale difference between two overlapping laser scans, the minimum number of linear features for the estimation of shifts and rotation angles are two non-parallel lines. Furthermore, short lines are not preferable for the registration process since their descriptive attributes are less accurate. As for the incorporation of linear features for the estimation of the transformation parameters, one could implement one of the following procedures: line-based approach (Habib et al., 2005) or point-based approach through a weight-modification process (Renaudin et al., 2011). These approaches are nonlinear and they require initial approximations of the transformation parameters, which are usually derived by roughly evaluating the position and orientation of the scans with respect to each other.

To eliminate the need for approximate parameters, we utilized the closed form approach that was proposed by Guan and Zhang (2011) for the estimation of the transformation parameters using linear features. Their approach uses unit quaternion to represent the rotation angles and hence it allows for the formation of a linear mathematical model. However, such a mathematical model is derived while assuming that conjugate linear features in two scans are in the same direction. This assumption would be applicable only if the linear features are manually matched. Therefore, we adapted this model to compensate for ambiguities that might result from potential direction variations among the hypothesized matches. To explain the conceptual basis of such mathematical model, suppose $\boldsymbol{n} = (n_x, n_y, n_z)$ and $\boldsymbol{N} = (N_x, N_y, N_z)$ are two unit vectors that represent conjugate lines in two different scans. Assuming that there is no scale variation between the two scans, a 3D rotation matrix (R) is required in order to align the vectors $\boldsymbol{n}$ and $\boldsymbol{N}$ to be parallel to each other (Equation 2). Since the minimum required number of linear features to estimate the three rotation angles is two, and assuming that we can identify two pairs of vectors that are pointing in the same direction similar to those shown in Figure 2 (i.e., $\boldsymbol{n}_1, \boldsymbol{n}_2$ and $\boldsymbol{N}_1, \boldsymbol{N}_2$). The least squares adjustment principle can be employed to estimate the unknown rotation matrix through minimizing the sum of squared residuals (SSR). Equation (3) represents the formation of the SSR based on the vectors observations.

$$\begin{bmatrix} N_x \\ N_y \\ N_z \end{bmatrix} = R \begin{bmatrix} n_x \\ n_y \\ n_z \end{bmatrix} \tag{2}$$

Figure 2. Pair of conjugate linear features that have similar direction vectors

$$\sum_{i=1}^{k} V_i^T V_i = \sum_{i=1}^{k} (R\boldsymbol{n}_i - \boldsymbol{N}_i)^T (R\boldsymbol{n}_i - \boldsymbol{N}_i) = \sum_{i=1}^{k} (\boldsymbol{n}_i^T \boldsymbol{n}_i + \boldsymbol{N}_i^T \boldsymbol{N}_i - 2\boldsymbol{N}_i^T R\boldsymbol{n}_i) \tag{3}$$

Where V_i is the associated residual for each conjugate line i, and k is the number of involved conjugate lines to estimate the rotation matrix.

The first two terms of Equation (3) (i.e., $\boldsymbol{n}_i^T \boldsymbol{n}_i$, and $\boldsymbol{N}_i^T \boldsymbol{N}_i$) are always positive as they are the squared magnitude of $\boldsymbol{n}_i$ and $\boldsymbol{N}_i$. Hence, in order to estimate the rotation matrix by minimizing the SSR, the term $\sum_{i=1}^{k} \boldsymbol{N}_i^T R\boldsymbol{n}_i$ has to be

maximized. Horn (1987) introduced a method to find the unit quaternion $\dot{q}$ corresponding to R that maximizes this term. Using quaternion properties, one can develop Equation (4).

$$\max_{R} \sum_{i=1}^{k} \boldsymbol{N}_i^T R \boldsymbol{n}_i = \max_{\dot{q}} \sum_{i=1}^{k} (\dot{q}\dot{\boldsymbol{n}}_i \dot{q}^*).\dot{\boldsymbol{N}}_i = \max_{\dot{q}} \sum_{i=1}^{k} (\dot{q}\dot{\boldsymbol{n}}_i).(\dot{\boldsymbol{N}}_i \dot{q}) = \max_{\dot{q}} \sum_{i=1}^{k} (\bar{C}_{\dot{\boldsymbol{n}}_i}\dot{q}).(C_{\dot{\boldsymbol{N}}_i}\dot{q})$$

$$\max_{\dot{q}} \sum_{i=1}^{k} \dot{q}^T \bar{C}_{\dot{\boldsymbol{n}}_i}^T C_{\dot{\boldsymbol{N}}_i}\dot{q} = \dot{q}^T \left(\sum_{i=1}^{k} \bar{C}_{\dot{\boldsymbol{n}}_i}^T C_{\dot{\boldsymbol{N}}_i} \right) \dot{q} = \dot{q}^T N \dot{q} \qquad (4)$$

The symbol ($\dot{}$) in Equation (4) denotes the quaternion form of a vector, which is nothing but adding a zero as the real part of quaternion (e.g., $\dot{\boldsymbol{N}}_i = (0, \boldsymbol{N}_i)$). According to Horn (1987), the C and $\bar{C}$ are 4×4 matrices that are used to convert quaternion-based multiplication to matrix-based multiplication. Matrix N is finally constructed from all the known vectors $(\boldsymbol{n}_i, \boldsymbol{N}_i)$. It has been proven that the eigen vector corresponding to the largest eigen value of N, is the unit quaternion that can be used to derive the rotation angles of R.

To estimate the rotation matrix R that maximizes the summation term $\sum_{i=1}^{k} \boldsymbol{N}_i^T R \boldsymbol{n}_i$, one should identify a conjugate pair of linear features in two scans while preserving consistent directions for each conjugate lines. The definition of the direction vectors for the extracted linear features within a laser scan is quite arbitrary and thus we cannot guarantee similar directions for conjugate pairs. In other words, for a pair of linear features ($\boldsymbol{n}_1$,$\boldsymbol{n}_2$) in one scan, four configurations are possible for its conjugate pair ($\boldsymbol{N}_1$,$\boldsymbol{N}_2$) as displayed in Figure 3.

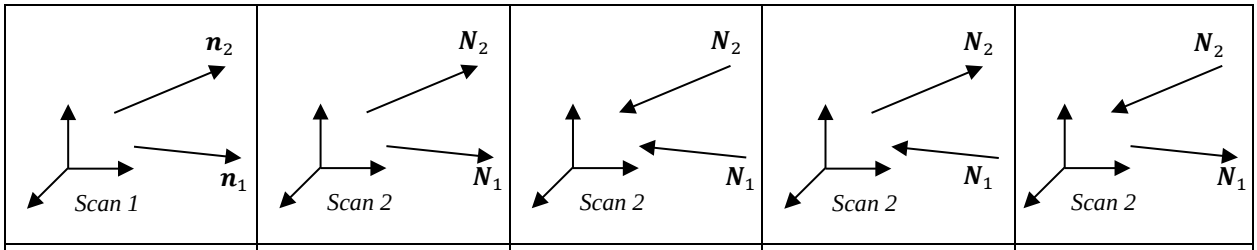

	Configuration 1	Configuration 2	Configuration 3	Configuration 4

Figure 3. Possible configurations of conjugate line pairs

We can establish theses configurations for any hypothesized conjugate pairs of linear features to solve for four rotation matrices. However, rather than considering all the configurations, and in order to reduce the number of investigated solutions, we classified the line pairs into three categories: (a) skew lines, (b) coplanar non-orthogonal lines, and (c) coplanar orthogonal lines.

(a) To reduce the number of possible configurations between hypothesized conjugate pairs of skew lines, we apply the following steps: first, we define the direction vectors of the involved lines in the first pair (e.g., vectors $\boldsymbol{n}_1, \boldsymbol{n}_2$ in Figure 4) in a way that their cross-product and their common perpendicular ($\vec{\boldsymbol{I}}$) will have compatible directions. Then, we determine which configuration of the second pair that has compatible directions for their cross product and common perpendicular (i.e., the common perpendicular from $\boldsymbol{N}_1$to $\boldsymbol{N}_2$ should be pointing in the same direction as the cross product $\boldsymbol{N}_1 \times \boldsymbol{N}_2$). As shown in Figure 4, the configurations 3 and 4 are filtered-out since their cross product direction is not compatible with the direction of the common perpendicular from $\boldsymbol{N}_1$to $\boldsymbol{N}_2(\vec{\boldsymbol{I}})$. Thereafter, we estimate two rotation matrices that will correspond to two opposite configurations (i.e., configurations 1 and 2). The first rotation matrix is derived using the eigen vector that correspond to the largest eigen value of the matrix N as mentioned earlier. To account for configuration 2, the rotation matrix is derived using the unit quaternion which is equal to the eigen vector corresponding to the smallest eigen value of matrix N. It should be noted that both rotation matrices are derived using the same matrix N.

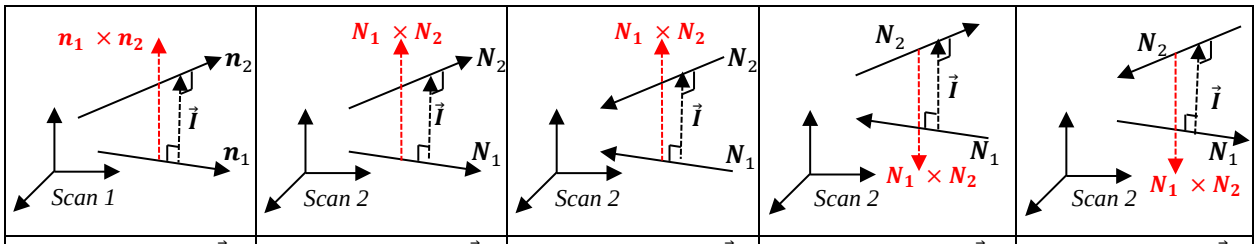

Dir ($\mathbf{n}_1 \times \mathbf{n}_2$) = Dir ($\vec{\mathbf{I}}$)	Dir ($N_1 \times N_2$) = Dir ($\vec{\mathbf{I}}$) Configuration 1	Dir. ($\mathbf{N}_1 \times \mathbf{N}_2$) = Dir ($\vec{\mathbf{I}}$) Configuration 2	Dir ($\mathbf{N}_1 \times \mathbf{N}_2$) ≠ Dir ($\vec{\mathbf{I}}$) Configuration 3	Dir ($\mathbf{N}_1 \times \mathbf{N}_2$) ≠ Dir($\vec{\mathbf{I}}$) Configuration 4

Figure 4. Direction comparison for the potential configurations of skew lines

(b) To reduce the number of possible configurations between hypothesized conjugate pairs of coplanar non-orthogonal lines, we apply the following steps: first, we define the direction vectors of the involved lines in the first pair in a way that they should form acute angle (e.g., vectors $\boldsymbol{n}_1, \boldsymbol{n}_2$ in Figure 5). Then, we determine which configuration of the second pair forms acute angle. In this case, configurations 3 and 4 are filtered-out. Thereafter, we estimate two rotation matrices that will correspond to two opposite configurations (i.e., configurations 1 and 2). For configuration 1, the eigen vector corresponding to the largest eigen value of the matrix *N* is the unit quaternion that define the unknown rotation matrix. On the other hand, the eigen vector corresponding to the smallest eigen value of the matrix *N* counts for configuration 2. Similar to skew line pairs, both rotation matrices are derived using the same matrix *N*.

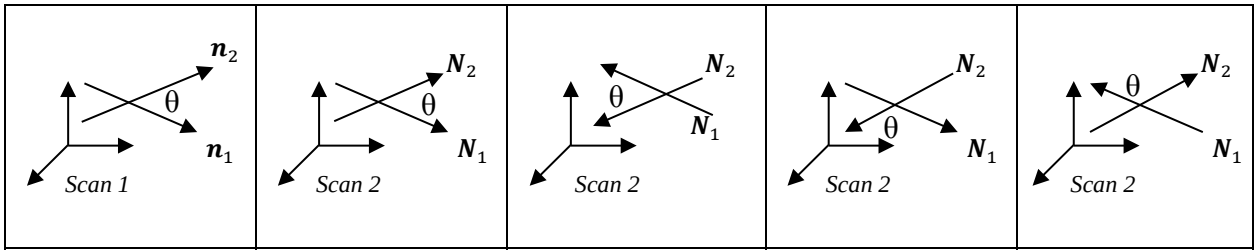

θ = acute angle	θ = acute angle Configuration 1	θ = acute angle Configuration 2	θ ≠acute angle Configuration 3	θ ≠acute angle Configuration 4

Figure 5. Angle check for potential configurations of non-orthogonal coplanar lines

(c) For hypothesized conjugate pairs of coplanar orthogonal lines, all the four configurations have to be considered since a pair of coplanar orthogonal vectors (e.g., $\boldsymbol{n}_1, \boldsymbol{n}_2$) would match any of the configurations shown in Figure 6. In this case, four rotation matrices have to be estimated. First, we derive two rotation matrices using the matching pair of linear features, which account for configurations 1 and 2. Then, we derive another two rotation matrices after changing the direction of one of the involved lines, which account for configurations 3 and 4. One should note that in this case two *N* matrices will be formed.

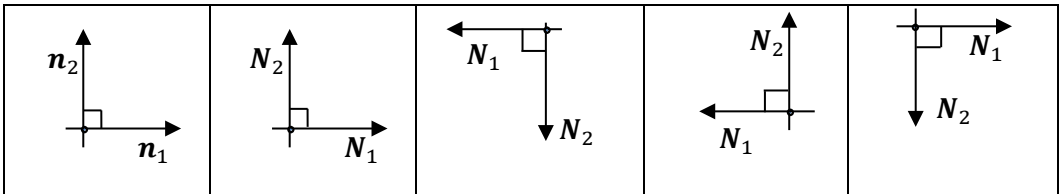

	Configuration 1	Configuration 2	Configuration 3	Configuration 4

Figure 6. Possible configurations of coplanar orthogonal vectors

Following the estimation of the rotation matrix, we can derive translation vector relating the scans if we can identify two conjugate points in the two scans being registered as in Equation5:

$$\begin{bmatrix} T_x \\ T_y \\ T_z \end{bmatrix} = \begin{bmatrix} P_x \\ P_y \\ P_z \end{bmatrix} - R \begin{bmatrix} p_x \\ p_y \\ p_z \end{bmatrix} \quad (5)$$

Where $T = (T_x, T_y, T_z)$ is the translation vector, $P = (P_x, P_y, P_z)$ and $p = (p_x, p_y, p_z)$ are conjugate points within the scans.

We have chosen the middle point of the common perpendicular line to a selected line pair in one scan as the conjugate to its equivalent for the selected line pair from the second scan. One should note that depending on the number of estimated rotation matrices, there will be equivalent number of corresponding translation vectors.

Determining the Most Frequent Set of Transformation Parameters

In order to solve for the transformation parameters relating two laser scans, any pair of linear features that is selected from the first scan is considered as a candidate match to another selected pair from the second scan if theses pairs have similar angular deviation and spatial separation values. By utilizing all the candidate matches to solve for the transformation parameters (i.e., each candidate match is used to solve for a single set of transformation parameters at a time), only the pairs representing correct matches would result in similar sets of transformation parameters. The degree of similarity between the estimated transformation parameters using the correct matches depends on the noise level in the data as well as the accuracy of the extracted lines. In other words, the derived transformation parameters from correct matches will not be perfectly identical. Hence, we need to identify a cluster of transformation parameters that are numerically close to each other. The process of identifying similar sets of transformation parameters requires an evaluation of six estimated values; namely, three translations (T_x, T_y, T_z) and three rotation angles $(\omega, \varphi, \kappa)$. In this regard, one could use a six dimensional Kd-tree data structure to store the six values. Since the spatial components (T_x, T_y, T_z) and the angular components $(\omega, \varphi, \kappa)$ of the transformation parameters would make it difficult for deriving an acceptable radius to encompass similar solutions, one can use two 3-dimensional Kd-tree structures, one for the rotation parameters, which is then followed by another one for the shift parameters. In this case, we can start by identifying compatible solutions in the $(\omega, \varphi, \kappa)$ kd-tree. Then, for the identified compatible solutions for the rotation-parameters, we can build another 3-dimensional Kd-tree for the shift parameters (i.e., the constituents of the Kd-tree for the shift parameters are the elements that correspond to the identified peak in the rotation Kd-tree). Finally, we identify the compatible solutions for the shift parameters within the respective kd-tree. However, identifying the most frequent solution might be sensitive to the selected radii for identifying similar solutions within the two Kd-tree data structures.

In this paper, we find similar sets of transformation parameters by using each set of transformation parameters to transform a specific 3D point (which is chosen to be the center of one of the scans) from the reference frame of one of the scans to the reference frame of the other one. It is assumed that similar transformation parameters will lead to a group of transformed points, which are spatially close to each other. A Kd-tree is used to store the transformed points and to identify the most common location of the transformed points (peak) and consequently the most probable solutions that lead to such points. One could argue that defining a meaningful radius for identifying compatible transformed points is much easier than defining the radii for compatible solutions in the rotation and translation Kd-tree data structures. Moreover, this approach would be much faster since we are dealing with a single Kd-tree data structure rather than two. Following the procedure of determining the most frequent set of transformation parameters, we use the average of these parameters as initial approximation for an ICPP registration process to achieve the fine alignment between the scans under consideration.

EXPERIMENTAL RESULTS

Experiments were conducted using a set of seven terrestrial laser scans. These scans were acquired over an electrical sub-station using the FARO Focus3D S scanner. As shown in Figure 7, the scanning mission is designed to have two central scans (i.e., scans 6 and 7) with significant overlap in between them (roughly 90%). The remaining five scans (i.e., scans 1, 2, 3, 4, and 5) are collected at the outer bounds of the field to fully cover the entire site. The outer scans have roughly 50% of overlap with the central scans.

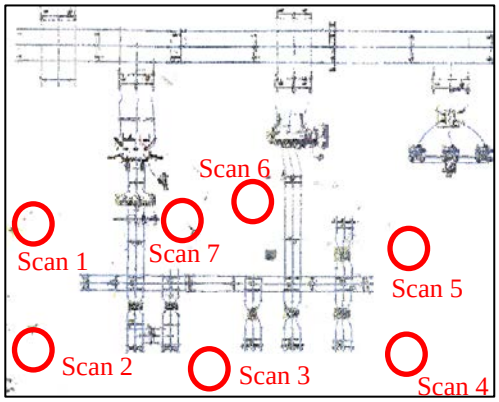

Figure 7. The distribution of the scanner locations within the sub-station

Pole-like features were extracted through the region-growing process to provide the experiment with the required linear features. Figure 8.a shows an example of the segmented pole-like features through the region-growing process for a part of the electrical sub-station. The points of each individual feature are projected onto the feature axis to define the lines (Figure 8.b).

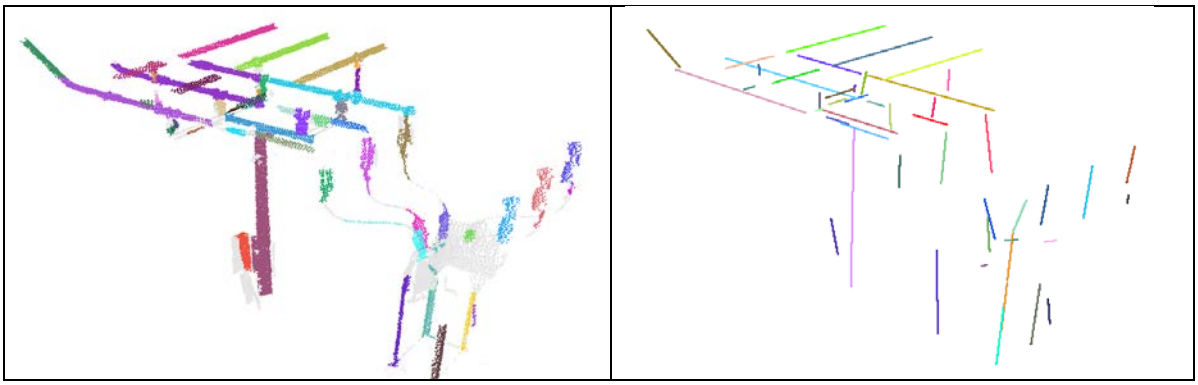

(a) (b)

Figure 8. The region-growing results for a part of the power plant: (a) segmented pole-like features, (b) derived line segments

We only selected long and precise pole-like features (e.g., linear features more than 1.0 m long with .05 m fitting precision), since those lines will have accurate attributes. Table 1 summarizes the number of extracted lines from each scan.

Table 1. The number of extracted lines from the different scans

Scan ID	Number of extracted lines
1	33
2	43
3	46
4	33
5	68
6	93
7	85

The laser scans were selected two at a time where scan 6 was always chosen as the reference scan. For a selected pair of scans, all the possible combinations of linear features are established. Then, the candidate matches of line pairs between the scans are identified as the ones which share similar angular deviation and spatial separation values. All the candidate matches – taken one at a time – are used to solve for the transformation parameters using the developed linear mathematical model. It should be noted that only the pairs that have angular deviation exceeding a predefined threshold (e.g., 35°) are considered. This condition is necessary to avoid selecting parallel pairs since such lines cannot be used to determine the shift along the lines' direction. For a selected pair of scans, all the estimated transformation parameters are used one at a time to transform the center point of one scan into the reference frame of the second scan. Thereafter, we determined the points that are spatially close to each other. Table 2 summarizes the solution frequency-based components for the scan pairs in question.

Table 2. Solution frequency-based components

Scans ID	Combinations	Candidate matches	Peak size
6-1	4,517,568	14,828	78
6-2	7,726,068	26,944	104
6-3	8,855,460	60,446	165
6-4	4,517,568	13,708	23
6-5	19,490,568	86,824	132
6-7	30,544,920	175,004	769

The number of combinations is the total number of possible matches of line pairs within the scans. The number of candidate matches represents the total number of line pairs from different scans that share similar angular deviation and spatial separation. All the candidate matches are used to solve for the transformation parameters. The peak size represents the number of transformed points that falls within a 0.20 m spherical radius in the transformed center-point Kd-tree. We calculated the average of the transformation parameters related to the points within the peak, and thereafter we used this average as the initial value to start the ICPP registration process. Table 3 summarizes the transformation parameters values from the peak averaging and ICPP outcome for all the experiments.

Table 3. Estimated transformation parameters between the scan pairs

Scans ID	Parameters source	T_x (m)	T_y (m)	T_z (m)	ω°	φ°	κ°
6-1	Peak averaging	6.317	-31.315	-0.051	-0.141	0.184	0.407
	ICPP	6.369	-31.290	-0.174	0.491	0.009	0.341
6-2	Peak averaging	28.350	-19.887	0.081	0.379	0.745	1.435
	ICPP	28.340	-19.859	0.069	0.388	0.740	1.457
6-3	Peak averaging	22.981	1.806	0.131	0.023	0.326	3.764
	ICPP	23.068	1.743	0.069	-0.024	0.397	3.665
6-4	Peak averaging	16.381	24.511	-0.075	-0.195	0.341	2.370
	ICPP	16.320	24.596	-0.058	-0.175	0.310	2.389
6-5	Peak averaging	-4.266	24.122	-0.136	-0.033	0.047	-4.685
	ICPP	-4.275	24.096	-0.098	0.0187	0.072	-4.641
6-7	Peak averaging	1.918	-9.067	-0.044	-0.179	-0.100	2.102
	ICPP	1.899	-9.052	-0.044	-0.083	-0.044	2.391

From Table 3, one can observe that the transformation parameters from both approaches (i.e., Peak averaging and the ICPP) are quite comparable for all the experiments. To investigate the quality of the estimated transformation parameters using both approaches, we display the registration result for a small part of scans four and six. This pair is selected since it shows the largest discrepancy in the estimated parameters from the different approaches. Figures 9.a and 9.b show a part of the registered scans using the peak-averaging transformation parameters and the ICPP transformation parameters, respectively. The features in red belong to scan four and the features in blue belong to scan six. For a better visualization of the registration results, Figures 10.a and 10.b display a cross-section over a single feature using the peak averaging transformation parameters and using the ICPP transformation parameters, respectively. Different colors indicate different scans.

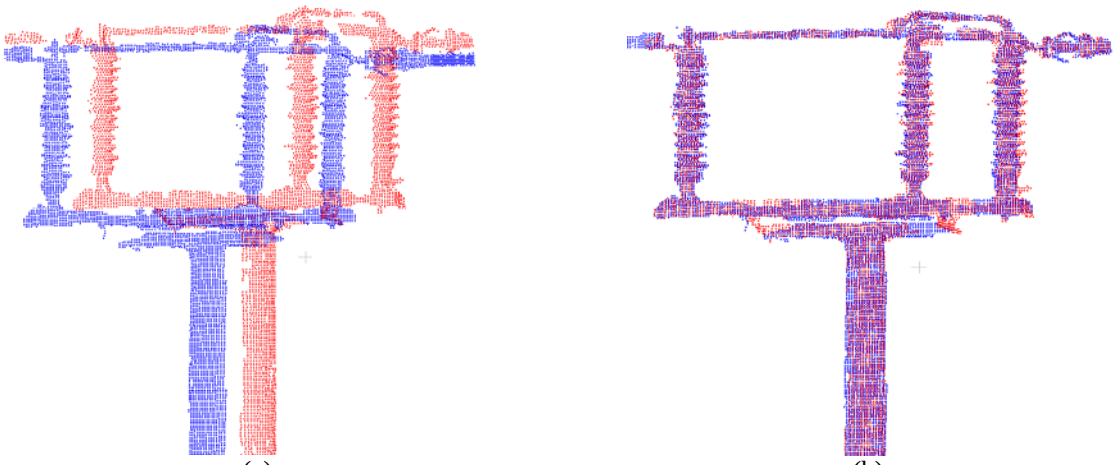

(a) (b)

Figure 9. Registration result for a part of electrical sub-station using the peak averaging transformation parameters (a), and registration using the ICPP transformation parameters (b)

(a) (b)

Figure 10. Cross- section over a single feature from an electrical-substation , after the registration using the peak averaging transformation parameters (a), and using the ICPP transformation parameters (b)

CONCLUSIONS AND RECOMMENDATIONS FOR FUTURE WORK

The paper outlined a new methodology for the automatic registration of overlapping terrestrial laser scans that contain plenty of conjugate linear features. We introduced a synergic combination of two registration methodologies (i.e., feature-based and point-based) to overcome the drawbacks of each method. Linear features were extracted from the scans using a region-growing approach. Angular deviation and spatial separation values were used to establish hypothesized conjugate pairs of linear features since these values are invariant to rotation and translation variation between the different scans. Utilizing an existing linear mathematical model for estimating the transformation parameters helped in avoiding the need for the initial approximations. Further modifications on the model helped to compensate for ambiguities resulting from potential direction variations among the hypothesized matches. The focus then moved to introducing several options to determine the most frequent set of transformation parameters, and there we recommended the use of the transformed center as the most convenient approach to check for the similarity between a set of available transformation parameters. To achieve the fine alignment between the overlapping scans through the ICPP, linear features provided the required approximates of transformation parameters. Finally, future work will focus on establishing the alignment between multiple scans at the same time using the frequency-based concept. We will employ dense-matching techniques to derive dense image-based point cloud. Thereafter, we will register images-based point cloud to a laser-based point cloud by utilizing the frequency-based approach.

ACKNOWLEDGMENT

This work was supported by the Natural Science and Engineering Council of Canada (NSERC-Discovery Grant), a Tecterra Grant (www.tecterra.com), and CANTEGA Grant ((www.cantega.com).

REFERENCES

Al-Durgham, M., Detchev, I., Habib, A., 2011. Analysis of two triangle-based multi-surface registration algorithms of irregular point clouds. Presented at the 2011 ISPRS Calgary 2011 Workshop, International Archives of the Photogrammetry, Calgary,Canada, pp. 61–66.

Asai, T., Kanbara, M., Yokoya, N., 2005. 3D modeling of outdoor environments by integrating omnidirectional range and color images, in: 3-D Digital Imaging and Modeling, 2005. 3DIM 2005. Fifth International Conference on. IEEE, pp. 447–454.

Besl, P., McKay, N., 1992. A Method for registration of 3-D shapes. Transactions on Pattern Analysis and Machine Intelligence 14(2), pp. 239–256.

Chen, Y., Medioni, G., 1992. Object modelling by registration of multiple range images. Image Vis. Comput. 10, 145–155.

Guan, Y., Zhang, H., 2011. Initial registration for point clouds based on linear features, in: Knowledge Acquisition and Modeling (KAM), 2011 Fourth International Symposium on. IEEE, pp. 474–477.

Habib, A., Detchev, I., Bang, K., 2010. comparative analysis of two approaches for multiple-surface registration of irrigular point clouds. Int. Arch. Photogramm. Sens. Spat. Inf. XXXVIII, 61–66.

Habib, A., Ghanma, M., Michel, M., Al-Ruzouq, R., 2005. Photogrammetric and LiDAR data registration using linear features. Photogramm. Eng. Remote Sens. 71(6), pp. 699–707.

Habib, A.F., Al-Ruzouq, R.I., 2004. Line-based modified iterated Hough transform for automatic registration of multi-source imagery. Photogramm. Rec. 19(105), pp. 5–21.

Horn, B.K., 1987. Closed-form solution of absolute orientation using unit quaternions. JOSA A 4, 629–642.

Jaw, J., Chuang, T., 2008. Feature-based registration of terrestrial lidar point clouds, in: International Archives of the Photogrammetry, Remote Sensing and Spatial Information Sciences (ISPRS). Beijing, China, pp. 303–308.

Lari, Z., Habib, A., 2013. A novel hybrid approach for the extraction of linear/cylindrical features from laser scanning data. ISPRS Ann. Photogramm. Remote Sens. Spat. Inf. Sci. II-5/W2, 151–156.

Liang, Y.-B., Zhan, Q.-M., Che, E.-Z., Chen, M.-W., Zhang, D.-L., 2014. Automatic Registration of Terrestrial Laser Scanning Data Using Precisely Located Artificial Planar Targets. IEEE Geosci. Remote Sens. Lett. 11, 69–73.

Matabosch, C., Salvi, J., Fofi, D., Meriaudeau, F., 2005. Range image registration for industrial inspection, in: Electronic Imaging 2005. International Society for Optics and Photonics, pp. 216–227.

Rabbani, T., van den Heuvel, F., 2005. Automatic point cloud registration using constrained search for corresponding objects, in: Proceedings of 7th Conference on Optical. pp. 3–5.

Renaudin, E., Habib, A., Kersting, A.P., 2011. Featured-based Registration of terrestrial laser scans with minimum overlap using photogrammetric data. ETRI J. 33, 517–527.

Roberts, K.S., 1988. A new representation for a line, in: Computer Vision and Pattern Recognition, 1988. Proceedings CVPR'88., Computer Society Conference on. IEEE, pp. 635–640.

Scaioni, M., 2005. Direct georeferencing of TLS in surveying of complex sites. Proc. ISPRS Work. Group 4, 22–24.

Yao, J., Ruggeri, M.R., Taddei, P., Sequeira, V., 2010. Automatic scan registration using 3D linear and planar features. 3D Res. 1(3), pp. 1–18.